Impacts of air pressure on the evolution of nanosecond pulse discharge products*

Yu Jin-Lu(于锦禄)[a)†], He Li-Ming(何立明)[a)], Ding Wei(丁 未)[b)], Wang Yu-Qian(王育虔)[a)], and Du Chun(杜 纯)[a)]

[a)] *The Engineering Institute, Air Force Engineering University, Xi'an* 710038, *China*
[b)] *Department of Training, Air Force Engineering University, Xi'an* 710051, *China*

(Received 10 April 2012; revised manuscript received 5 September 2012)

Based on the nonequilibrium plasma dynamics of air discharge, a dynamic model of zero-dimensional plasma is established by combining the component density equation, the Boltzmann equation, and the energy transfer equation. The evolution properties of nanosecond pulse discharge (NPD) plasma under different air pressures are calculated. The results show that the air pressure has significant impacts on the NPD products and the peak values of particle number density for particles such as O atoms, O_3 molecules, N_2(A3) molecules in excited states, and NO molecules. It increases at first and then decreases with the increase of air pressure. On the other hand, the peak values of particle number density for N_2(B3) and N_2(C3) molecules in excited states are only slightly affected by the air pressure.

Keywords: plasma, air pressure, evolution, numerical simulation

PACS: 52.25.Jm, 52.25.Dg, 52.65.−y, 34.50.Ez **DOI:** 10.1088/1674-1056/22/5/055201

1. Introduction

Physical and chemical properties of gas discharge plasma (GDP) during the discharge process enable GDP to be extensively applied in plasma applications like etching, film coating, drag reduction, combustion, and laboratory plasma.[1–4] In the aerospace field, the use of gas discharge to intensify combustion has shown unique advantages[5] in applications such as improving the reliability of re-ignition of aero-engines in the sky, reducing the ignition delay time of pulse detonation engines (PDE),[6,7] scramjet engines,[8,9] and decreasing the production of NO_x under the fuel-lean burn.[10,11]

Although the classic Townsend mechanism and stream theory are the basis of research on gas discharge, they have some defects when used to explain nanosecond pulse gas discharge. Under normal pressure and high pressure, many low-pressure plasma diagnostic methods, such as the Langmuir probe, are useless. Some diagnostic approaches, such as the spectral line broadening of the Stark effect and Thomson scattering, are limited by the precision of instruments and by the manufacturing cost of equipment, so they cannot be used for common laboratory diagnosis and industrial diagnosis. This makes many basic features and time characteristics of atmosphere and high-pressure plasmas inaccessible to experimental measurements. Therefore, mathematical modeling and computer numerical simulation become major methods of exploring and optimizing the gas discharge process.

Shao *et al.*[12] studied the runaway process and collision ionization of fast electrons by numerical simulations. Nissen *et al.*[13] put forward a temporal evolution model of the chemical process for dielectric barrier discharge, in which a gas mixture including N_2, O_2, H_2O, NO, NO_2, and C_2H_4 was concerned. They also compared the calculated results with the experimental results. Mintusov *et al.*[14] studied the intensified combustion effect and the dynamic computation model for high-voltage nanosecond repeated pulse discharge. Shi *et al.*[15] studied the glow discharge in pure helium gas at the pressure of 1.333×10^3 Pa under a high-voltage nanosecond pulse by numerical simulations. Uddi *et al.*[16] investigated the chemical reaction rate for repeated discharge. Meanwhile, Shibkov *et al.*[17] studied the ignition temperature rise time for a hydrogen–oxygen mixture under the condition of non-equilibrium air discharge plasma. Kosarev *et al.*[18] studied the ignition mechanism for CH_4/O_2/Ar mixture in nanosecond pulse discharge by means of experiments and numerical simulations, showing that the ignition of nanosecond pulse discharge plasmas can shorten ignition delay time effectively.

Although there have been some achievements in research on the discharge characteristics of nanosecond pulse discharge, it is necessary for researchers to learn the underlying nature of nanosecond pulse discharge sufficiently so that it can be better applied in industry. Currently, the investigations on nanosecond gas discharge are still in the exploratory stage.

However, previous studies have mostly concentrated on plasma under low pressure, even though plasma is often used in high-pressure ($>$ 1 atm, 1 atm $= 1.01325 \times 10^5$ Pa) environments in application fields such as plasma enhanced combustion and plasma flow control.[4–11]

*Project supported by the National Natural Science Foundation of China (Grant Nos. 51106179 and 51276196).
†Corresponding author. E-mail: yujinlu1@163.com
© 2013 Chinese Physical Society and IOP Publishing Ltd

Therefore, research on nanosecond pulse discharge under air pressure conditions is necessary. This paper reports our study of the evolution of discharge particle number density in the air with changing air pressure by combining the component density equation, the Boltzmann equation, and the energy transfer equation. The calculated results in this paper can be used as a reference for research on the assisted combustion and the parameter control of plasmas.

2. Dynamical model of air discharge

The plasma dynamic model consists of elastic collision, excitation, ionization, electron adsorption/desorption, recombination, etc. For convenience in calculation, spatial processes like diffusion and drifting are neglected.

2.1. Component density equation[16]

For chemical reactions, we have

$$\sum_{i(\text{react})} a_i A_i \underset{k_\text{r}}{\overset{k_\text{f}}{\Leftrightarrow}} \sum_{j(\text{prod})} b_j B_j, \tag{1}$$

where k_f is the forward reaction rate coefficient, k_r is the backward reaction rate coefficient, A_i and B_j are the reactant and the product of the chemical reaction, and a_i and b_j are stoichiometric coefficients of component i and j, respectively. The reaction rate R is

$$R = k_\text{f} \prod_{i(\text{react})} n_i^{a_i} - k_\text{r} \prod_{j(\text{prod})} n_j^{b_j}. \tag{2}$$

The corresponding Arrhenius Form is

$$k_\text{f} = AT^n \exp\Big(-\frac{E_\text{A}}{RT}\Big), \tag{3}$$

where A is the prefactor, T is the temperature, n and E_A refer to the constant and the activation energy. In the computation model, the variation rate of component density in Eq. (1) is

$$\Big(\frac{\mathrm{d}n_j}{\mathrm{d}t}\Big)_\text{chem} = (b_j - a_j)R, \tag{4}$$

where n_j is the particle number density of component j. A corresponding reaction rate equation for each species in the elementary reactions of the reaction system is established, which can be reduced to the initial-value problem of the first-order ordinary differential equations relating the corresponding species density to study the temporal evolution of each species. The thermochemical data of chemical components required by Eq. (4) can be obtained by using CHEMKIN thermochemical data by means of segmentation computation. In this way, the differential equations of chemical reaction dynamics can be established and solved.

2.2. Boltzmann equation[16]

The reaction rate constant of the electron-molecule collision can be obtained via normalizing the electron energy distribution function derived by solving the Boltzmann equation using the chasing method. With the effect of steady electric field on homogeneous gas, the Boltzmann equation of an electron is

$$\frac{-eE}{m} \cdot \nabla_v f(\boldsymbol{v}) = \Big(\frac{\delta f(\boldsymbol{v})}{\delta t}\Big), \tag{5}$$

where e, m, v, and E are electron charge, mass, velocity, and electric field intensity, respectively. While $f(\boldsymbol{v})$ is the electron velocity distribution function. Let the electron energy $u = mv^2/2e$. Because the number of particles in excited states in the gas is quite small compared with the total number of particles, the hyper-elastic collision is neglected. Thus, the static Boltzmann equation can be obtained

$$\begin{aligned} &-\frac{1}{3}\Big(\frac{E}{N}\Big)^2 \frac{\mathrm{d}}{\mathrm{d}u}\Big\{u\frac{\mathrm{d}f_0(u)}{\mathrm{d}u}\Big[\sum_j N_j Q_{ej}(u)\Big]^{-1}\Big\} \\ &= \sum_i \frac{2m}{M_i}\frac{\partial}{\partial u}\Big[u^2 Q_{\text{T}_i}(u)\Big(f + \frac{kT}{e}\frac{\partial f}{\partial u}\Big)\Big] \\ &\quad + \sum_i B_i \frac{\partial}{\partial u}\Big[uQ_{\text{T}_i}(u)\Big(f + \frac{kT}{e}\frac{\partial f}{\partial u}\Big)\Big] \\ &\quad \sum_k \big[Q_k(u+u^*)f(u+u^*)(u+u^*) - Q_k(u)f(u)(u)\big], \end{aligned} \tag{6}$$

where $Q_{ej}(u)$ is the elastic collision cross-section of the electron, $Q_{\text{T}_i}(u)$ is the collision cross-section of the electron rotation, $Q_k(u)$ is the collision cross-section of electron excitation,[19–21] M is the mass of the molecule, B is the coefficient of rotation effect, and $f(u)$ is the distribution function of electron energy. Electron collision cross-sections of elastic collisions and inelastic collisions (such as vibration, electron excitation, and ionization) can be used as the input for solving Boltzmann equation. Then, the second-order difference method is used to solve the Boltzmann equation to get the electron energy distribution function $f(u)$. Finally, the reaction rate coefficient in the process of electron collisions can be calculated by

$$k = \Big(\frac{2e}{m_\text{e}}\Big)^{1/2} \int Q(u) u f(u) \mathrm{d}u, \tag{7}$$

where m_e is the mass of the electron.

2.3. Energy transfer equation

The energy equation[4] describing temperature variations in the system adopted can be approximated by the adiabatic isochoric equation, that is

$$\frac{N}{\gamma - 1}\frac{\mathrm{d}T}{\mathrm{d}t} = \sum_{j=1}^{j_\text{max}} \pm\delta\varepsilon_j R_j + P_\text{elast}[N_e], \tag{8}$$

where N is the particle number density, γ is the gas adiabatic index, $\delta\varepsilon$ is the heat released in chemical reactions, R is the speed of chemical reactions, P is the energy of electron rotation, and N_e is the electron concentration. The first item on the right stands for the heat released in chemical reactions, and the second item represents the Joule heat resulting from electron current and from elastic collisions between electrons and

heavy particles. As the transfer rates of positive ions and anions are relatively slow compared with that of electrons, the Joule heat caused by ion current is neglected.

The chemical reactions of plasma discharge include 49 excitation-ionized air components (Table 1) and 302 equations. The reaction rate constant of electron–molecule collision can be obtained by normalizing the electron energy distribution function, which can be obtained by solving the Boltzmann equation using the chasing method.

Table 1. Components of reactant.

Type	Components	Kinds
Nitrogen particle	N, N_2, N_2(v1), N_2(v2), N_2(v3), N_2(v4), N_2(v5), N_2(v6), N_2(v7), N_2(v8), N_2(A3), N_2(B3),N_2(a‘1), N_2(C3), N(2D), N(2P), N^+, N_2^+, N_3^+, N_4^+	20 kinds
Oxygen particle	O_2, O_2(v1), O_2(v2), O_2(v3), O_2(v4), O_2(a1), O_2(b1), O_2(4.5eV), O, O(1D), O(1S), O_3, O+, O_2^+, O_4^+, O^-, O_2^-, O_3^-, O_4^-	19 kinds
Compound particle	NO, NO^+, NO^-, NO_2, N_2O, NO_3, N_2O_4, N_2O_5, $O_2N_2^+$	9 kinds
Electron	e	1 kind

3. Calculated results and discussion

In the calculations, the discharge time is set as 35 ns, which is the discharge time of nanosecond pulse power in our laboratory. The initial temperature of air is set as 300 K and the ratio of N_2 to O_2 is 4:1. The research objects are chosen to be O atoms, O_3 molecules, N_2 (A3, B3, C3) in the excited states of nitrogen, and NO particles. They have significant impacts on the process of intensified combustion. The evolution of discharge products with time is analyzed.

3.1. Oxygen particles

When the reduced electric field is 100 Td (1 Td = 10^{-17} V·cm^2), the evolution of particle number density for O atoms versus time is shown in Fig. 1.

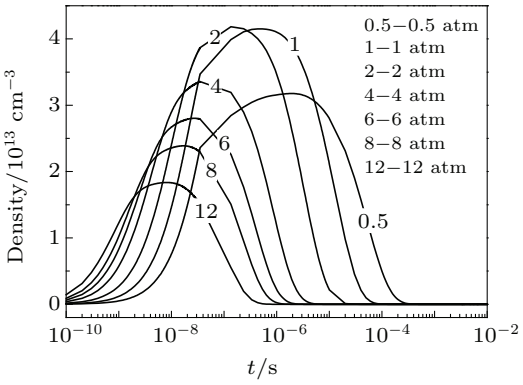


Fig. 1. Evolution of particle number density for O atoms with time.

The peak value and peak time of particle number density for O atoms are closely related to the air pressure. The peak value of O atoms concentration first increases and then decreases with gas pressure. When the gas pressure is 0.5 atm, the peak value of particle number density is 3.18×10^{-13} cm^{-3}. When the gas pressure is 1 atm and 2 atm, the peak value increases to 4.15×10^{-13} cm^{-3} and 4.18×10^{-13} cm^{-3}, respectively. As the gas pressure increases continuously, the peak value of O atoms concentration decreases. When the gas pressure is 12 atm, the peak value of particle number density for O atoms is 1.86×10^{-13} cm^{-3}.

This indicates that if the gas temperature and the electric-field intensity in the discharge area are both invariant, the peak value of the particle number density for O atoms produced by discharge under a certain gas pressure ($p_{\mathrm{O\,max}} \approx 2$ atm) will achieve its maximum. When the gas pressure is lower than 2 atm, the peak value of particle number density for O atoms increases as the gas pressure increases; and the lower the pressure is, the more time needed to reach the peak value. This complies with the experimental measurement results in Ref. [22]. When the gas pressure is higher than 2 atm, the peak value of particle number density for O atoms decreases as the gas pressure increases. This is because the particle number density within a unit area increases and the mean free path of charged particles shortens as the gas pressure increases ($P > P_{\mathrm{O\,max}}$) under constant gas temperature and reduced electric field intensity. This makes the energy obtained by the charged particles in free path decrease, which is unfavorable for the discharge and decreases the particle number density of O atoms.

After the particle number density of O atoms achieves the peak value, it begins to decrease. If the gas pressure is different, the time needed for the particle number density of O atoms to achieve the peak value is different and the decay time is also different. The higher the gas pressure is, the shorter the time needed for the particle number density of O atoms to achieve the peak value is and the short the decay time is. While, the lower the gas pressure is, the longer the time needed for the particle number density of O atoms to achieve the peak value is and the longer the decay time is. According to Paschen's Law, the possible reason is that the higher the gas pressure, the larger the number of times elastic electron collision occurs and the more energy is lost by electrons. This is unfavorable for the generation of collision ionization. Thus, the particle number density decreases.

The evolution relationship between the particle number density of O_3 molecules and time is shown in Fig. 2. Comparing Fig. 1 with Fig. 2, we find that the time when the particle number density for O atoms decreases is in accord with the time when the particle number density for O_3 ozone molecules increases. This shows that O atoms decay by the reaction ($O + O_2 + M \Rightarrow O_3 + M$). Hence, with the increase of gas pressure, the particle number density of O atoms increases at first and then decreases, and so does the particle number density of O_3 molecules.

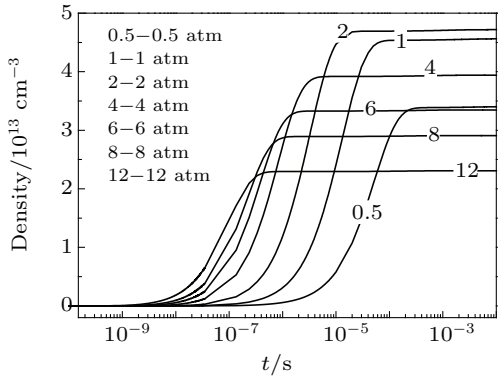


Fig. 2. Evolution of particle number density for O_3 molecules with time.

In Table 2, it is shown that the particle number density of O atoms changes as the pressure changes under different reduced electric fields. The peak value of the particle number density for O atoms increases as the reduced electric field increases under the same pressure. This is because when the pressure and temperature in the discharge area remain constant, the improvement of the reduced electric field, i.e., the improvement of the electric-field intensity in the discharge area, means the energy injected into the discharge area increases and the average electron energy increases. Thus the reaction rate coefficient for electron collisions improves and the reaction rate of particle collisions producing active particles also improves. The concentration of active particles increases, that is, the particle number density of O atoms increases. Under a certain reduced electric field, when gas pressure increases to 12 atm from 5 atm, there is gas pressure that can result in the peak value of particle number density for O atoms. When the reduced electric field is 50 Td, 75 Td, and 100 Td, the pressures at which the peak value of the particle number density for O atoms achieves maximum are all 2 atm. When the reduced electric field increases to 125 Td, the pressure at which the peak value of the particle number density for O atoms achieves maximum increases to 6 atm. This means more O atoms can be obtained under higher pressures, because the energy injected into the discharge area increases.

Table 2. The maximum of particle number density for O atoms (unit: 10^{13} cm^{-3}).

Press/atm	Reduced electric field/Td			
	50	75	100	125
12	0.003496	0.46042	1.83534	129.435
8	0.005279	0.63195	2.38806	2701.11
6	0.007025	0.77283	2.8031	3886.08
4	0.103185	0.98406	3.35614	2058.45
3	0.129396	1.12134	3.71106	919.222
2	0.165669	1.32534	4.18327	260.493
1	0.143098	1.29702	4.15125	55.6694
0.5	0.008.676	0.93935	3.17682	16.4289

3.2. Nitrogen particles

When the reduced electric field is 100 Td, the evolution of the particle number density for nitrogen molecules N_2 (A3) in excited states versus time is shown in Fig. 3.

The peak value and peak time of particle number density for N_2 (A3) particle are closely related to the air pressure. When the gas pressure increases to 12 atm from 0.5 atm, the peak value of the particle number density for N_2 (A3) particles increases at first and then decreases as the air pressure increases. When the gas pressure is 1.0 atm, the peak value of the particle number density for N_2 (A3) particles achieves the maximum value 3.05642×10^{-12} cm^{-3}. The gas pressure at which the peak value of the N_2 (A3) particle number density reaches its maximum is different from that of O atoms and O_3 molecules.

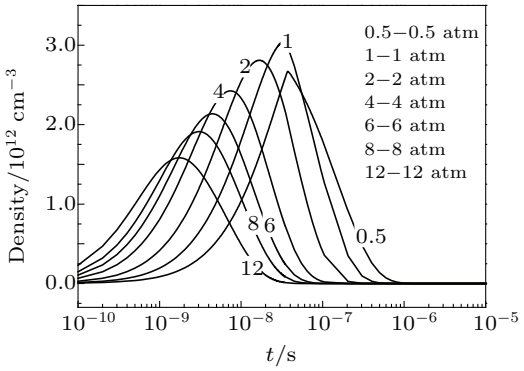


Fig. 3. Evolution of particle number density for N_2 (A3) with time.

The evolution of the particle number density for N_2 (A3) and N_2 (C3) versus time is shown in Figs. 4 and 5, respectively. From the two figures, it is found that when the gas pressure increases to 12 atm from 0.5 atm, the peak value of particle number density for N_2 (A3) and N_2 (C3) changes slightly with the increase of the gas pressure. However, the peak time is different. The higher the gas pressure, the shorter the peak time; the lower the gas pressure, the longer the peak time. When the discharge end time 35 ns comes, N_2 (A3) and N_2 (C3) particles have almost finished their decay.

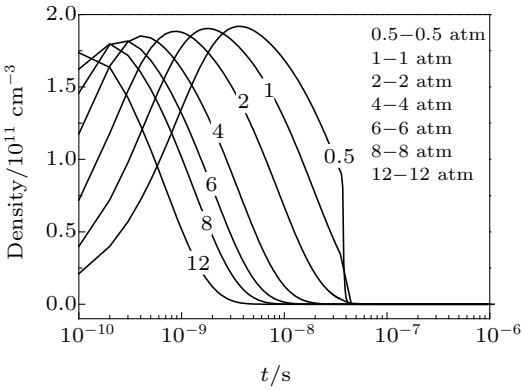


Fig. 4. Evolution of particle number density for N_2 (B3) with time.

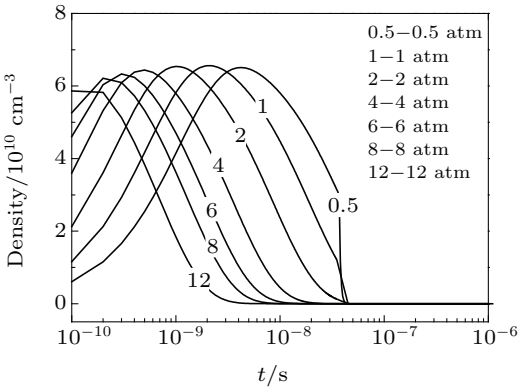


Fig. 5. Evolution of particle number density for N_2 (C3) as time changes.

Meanwhile, O atoms can be obtained by a collision/dissociation reaction between excited nitrogen molecules N_2 (A3, B3, C3, a‘1) and O_2 molecules. The collision reaction process is

$$N_2(A_3) + O_2 \Rightarrow N_2 + O + O, \tag{9}$$

$$N_2(B_3) + O_2 \Rightarrow N_2 + O + O, \tag{10}$$

$$N_2(C_3) + O_2 \Rightarrow N_2 + O + O(1S), \tag{11}$$

$$N_2(a‘1) + O_2 \Rightarrow N_2 + O + O. \tag{12}$$

From Figs. 3–5, it is found that the particle number densities of N_2 (A3), N_2 (B3), and N_2 (C3) are very low. The maximal particle number density of N_2 (A3), which is the highest among the three excited nitrogen molecules, is smaller than that of O atoms by one order of magnitude. Moreover, the three excited nitrogen molecules decay rapidly. Although the increase time of the number density of N_2 (A3), N_2 (B3), and N_2 (C3) is the same as that of O molecules, they do not play leading roles in the process of producing O atoms because of their low particle number density.

3.3. NO particles

The evolution of the particle number density for NO versus time is shown in Fig. 6, in which there are two rapid increasing gradients for the particle number density of NO. This is in accordance with the experimental results in Ref. [16].

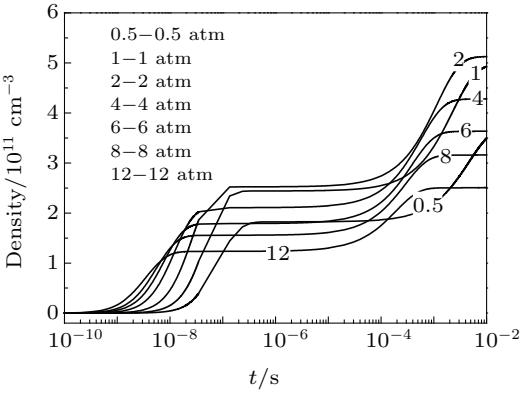


Fig. 6. Evolution of the particle number density for NO with time.

The time at which the particle number density of NO increases for the first time is $\sim$ μs. NO is mainly produced by the reaction between N (2D) /N (2P) and O_2, and soon later the balance level is achieved. The time at which the particle number density of NO increases for the second time is about ms. NO is produced by the reaction between N atoms and O_2.

The particle the number density of NO changes as the gas pressure changes. When the gas pressure increases for the first time, the particle number density of NO, largest at 2 atm, increases at first and then decreases as the gas pressure increases to 12 atm from 0.5 atm. When the gas pressure is 12 atm, the particle number density of NO balances at first. The evolution is similar to that of O atoms as time changes. The evolution for the second increase gradient of the NO particle number density is similar to that for the first increase gradient.

4. Conclusion

Based on the non-equilibrium plasma dynamics of gas discharge, a dynamical model of zero-dimensional plasma is established by combining the component concentration equation, the Boltzmann equation, and the energy transfer equation. The evolution of plasma concentration versus time under different air pressures are obtained by solving the dynamic model. The calculated results show as follows.

(i) With the increase of the gas pressure, there is a certain pressure $P_{\mathrm{O}\max}$ ($P_{\mathrm{O}\max} \approx 2$) atm under which the peak value of particle number density for O atoms in the discharge is the largest. When the gas pressure is lower than $P_{\mathrm{O}\max}$, the peak value of the particle number density for atom O increases with the gas pressure. The peak time for O atoms appears and the decay time also increases. When the gas pressure is higher than $P_{\mathrm{O}\max}$, the peak value of particle number density for O atoms decreases with the increase of gas pressure, the peak time for O atoms appears and the decay time shortens.

(ii) The evolutions of O_3 molecules, NO particles, N_2 (A3), and O atoms are basically the same. However, for N_2 (A3) particles, the gas pressure under which the peak value of the particle number density is the largest is different from those of O atoms, O_3 molecules, and NO particles. This shows that the gas pressure at which the peak value of the particle number density is achieved is different for different particles.

(iii) The peak values of the particle number densities for N_2 (B3) and N_2 (C3) change slightly as the gas pressure increases. However, the time at which their peak values appear is different. The higher the gas pressure is, the shorter the peak time is; the lower the gas pressure is, the longer the peak time is.

Acknowledgment

The authors would like to express their gratitude to Du Hong-Liang of the Air Force Engineering University, China.

References

[1] Li Y H 2011 *Advances in Aeronautical Science and Engineering* **2** 127 (in Chinese)

[2] Lan Y D, He L M, Ding W and Wang F 2010 *Acta Phys. Sin.* **59** 2617 (in Chinese)

[3] Lü Y, Chen X M, Cao Z R and Wu W D 2010 *Acta Phys. Sin.* **59** 3892 (in Chinese)

[4] Ding W, He L M and Song Z X 2010 *High Volt. Engin.* **36** 745 (in Chinese)

[5] Starikovskaia S M 2006 *J. Phys.* D: *Appl. Phys.* **39** 265

[6] Wang F, Jiang C, Kuthi A and Gundersen M A 2004 *AIAA*-2004-834. 42*nd AIAA Aerospace Sciences Meeting and Exhibit*, January 5–8, 2004, Reno, Nevada

[7] Cathey C, Wang F and Tang T 2007 45*th AIAA Aerospace Sciences Meeting and Exhibit*, January 8–11, 2007, Reno, USA, p. 443

[8] Mozingo J A 2004 *Evaluation of a Strut-Plasma Torch Combination as a Supersonic Igniter-Flameholder* (Ph. D dissertation) (Virginia: Virginia Polytechnic Institute and State University)

[9] Sergey L, Dmitry Y and Campbell C 2009 *J. Propul. Power* **25** 289

[10] Charles D C, Tao T, Taisuke S and Tomonori U 2007 *IEEE Trans. Plasma Sci.* **35** 1664

[11] Liu J B, Ronney P D and Wang F 2003 41*st AIAA Aerospace Sciences Meeting and Exhibit*, January 6–9, 2003, Reno, NV, p. 877

[12] Shao T, Sun G S and Yan P 2006 *Acta Phys. Sin.* **55** 5964 (in Chinese)

[13] Niessen W, Wolf O and Schruft R 1998 *J. Phys. D: Appl. Phys.* **31** 542

[14] Mintusov E, Serdyuchenko A and Choi I 2008 46*th AIAA Aerospace Sciences Meeting and Exhibit*, January 7–10, 2008, Reno, NV, p. 1106

[15] Shi F, Zhang L L and Wang D Z 2009 *Chin. Phys. B* **18** 1177

[16] Uddi M 2008 *Non-Equilibrium Kinetic Studies Of Repetitively Pulsed Nanosecond Discharge Plasma Assisted Combustion* (Ph. D dissertation) (Ohio: Ohio State University)

[17] Shibkov V M and Konstantinovskij R S 2005 43*rd AIAA Aerospace Sciences Meeting and Exhibit*, January 10–13, 2005, Reno, NV, p. 987

[18] Kosarev I N, Aleksandrov N L, Kindysheva S V and Starikovskaia S M 2008 *Combust. Flame* **154** 569

[19] Itikawa Y, Hayashi M, Ichimura A, Onda K, Sakimoto K, Takayanagi K, Nakamura M, Nishimura H and Takayanagi T 1986 *J. Phys. Chem. Ref. Data* **15** 985

[20] Itikawa Y, Ichimrua A and Onda K 1989 *J. Phys. Chem. Ref. Data* **18** 23

[21] Phelps A V and Pitchford L C 1985 *Phys. Rev. A* **31** 2932

[22] Uddi M, Jiang N, Mintusov E, Adamovich I V and Lempert W R 2008 46*th AIAA Aerospace Sciences Meeting and Exhibit*, January 7–10, 2008, Reno, NV, p. 1110